1.9 THE INFLUENCE OF LATENT HEAT RELEASE ON THE OCCLUSiON PROCESS IN AN IDEALIZED PRIMITIVE EQUATION SIMULATION

Jonathan E. Martin*, Derek J. Posselt, and Justin McLay
University of Wisconsin-Madison
Madison, WI 53706

1. Introduction

The canonical warm occluded thermal structure consists of an axis of maximum θ_e extending from the surface to the tropopause between two adjoining baroclinic zones. The axis of maximum θ_e is characterized by locally weak stratification and often bears a strong relationship to the heavy precipitation commonly found in the occluded quadrant of cyclones. Prior observational work by Martin (1998) has identified a characteristic tropopause-level PV signature, termed the PV treble clef, to be a sufficient condition for asserting the presence of a warm occluded thermal structure in the underlying troposphere. In a recent paper, Posselt and Martin (2003) exploited this relationship in order to investigate the influence of latent heat release (LHR) on the development of the occluded thermal structure in an observed cyclone. In the present paper, we conduct a more general examination of the role of LHR in the production of occluded thermal structures by employing companion full physics and dry numerical simulations performed using the idealized version of the University of Wisconsin Non-hydrostatic Modeling System (UW-NMS) model. In Section 2 we describe the specifications of the model employed in this study, as well as the experimental design. Preliminary results from the two simulations are contrasted in section 3, illustrating the fact that marked differences exist between the full physics and no-LHR idealized simulations.

2. The idealized UW-NMS

The simulations used in this study were carried out using a channel model version of the UW-NMS (Tripoli 1992) employing an analytic initialization scheme based upon formulations by Fritsch et al. (1980), Nuss and Anthes (1987) and Cao and Cho (1995) as modified by B. Hoggatt. The simulations were run on a spherical grid with resolution 126 x 100 km at the equator over a domain 5800 x 6000 km centered at 38°N. Forty vertical levels were used with Δz starting at 300 m and stretching to 600 m above the first 12 grid levels. The model top (at 20.5 km) included a Rayleigh friction zone while the bottom was flat and homogeneous with a Businger surface layer. A first order turbulence closure scheme was used along with full microphysics and a version of the Emanuel (1991) cumulus parameterization (in the full physics case). The initialization specifies a zonal jet with a 4000 km moderate amplitude sinusoidal perturbation in temperature and pressure imposed upon it, and the integrations were run for 96 h. One integration was run with a complete suite of model physics (the full physics, or FP, run) while another was run without a cumulus parameterization and with all temperature tendency terms arising from phase change of the water substance set to zero (the no-LHR, or NLHR, run).

3. Preliminary results

The 9 km potential vorticity (PV) at 42 h into the NLHR integration is presented in Fig. 1a. Some tendency for a local tropopause-level PV minimum is noted north of the Great Lakes. The associated sea-level pressure minimum is located over southern Wisconsin and has a well-developed lower tropospheric thermal ridge wrapped up into it at this time (Fig. 1b). A vertical cross-section of θ_e along line A-A' in Fig. 1b is shown in Fig. 1c. An axis of maximum θ_e is discernible in the section though it is not particularly robust.

Output from the companion full physics simulation is shown in Fig. 2. Note the much better developed tropopause PV minimum in the full physics case (Fig. 2a) with PV values less than 2 PVU extending over much of northern

*Corresponding author address: J. E. Martin, Univ. of Wisconsin-Madison, Dept. of Atm. And Oceanic Sciences, Madison, WI 53706; e-mail: jon@aos.wisc.edu.

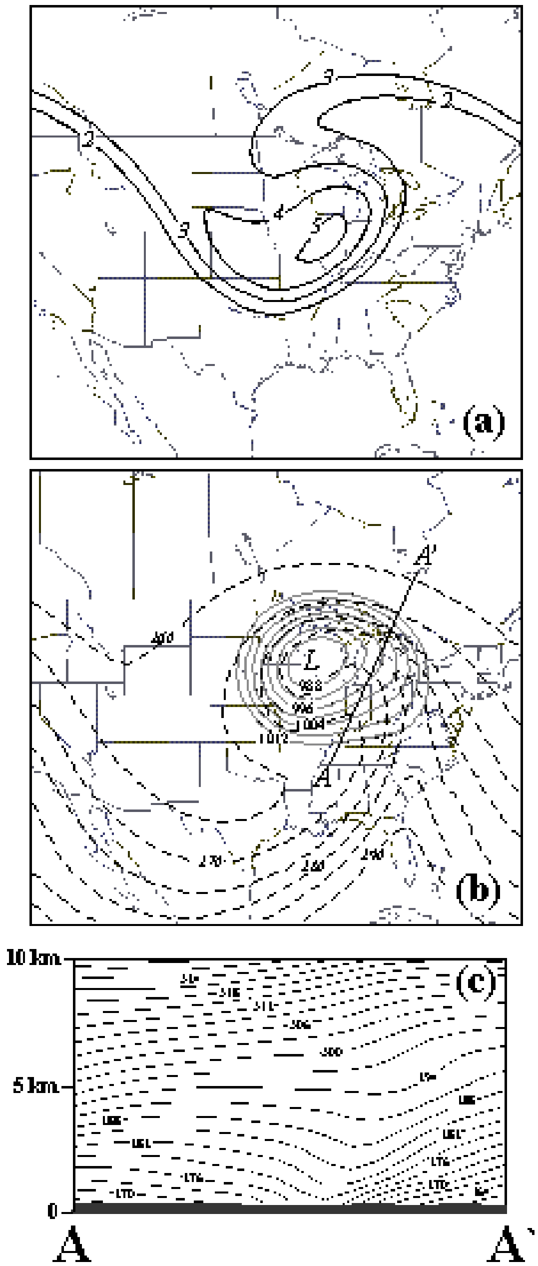

Fig. 1 (a) 9 km PV at 42 h in the NLHR simulation. PV labeled in PVU and contoured every 1 PVU beginning at 1 PVU. (b) Sea-level isobars (thick gray lines) and 300 m θ_e (dashed lines) at 42 h in the NLHR simulation. Isobars labeled in hPa and contoured every 4hPa equal to and below 1012 hPa. θ_e labeled in K and contoured every 5 K. (c) Vertical cross-section along line A-A' in Fig. 1b of θ_e. θ_e labeled in K and contoured every 3 K.

Minnesota, and an underlying 300 m θ_e ridge that is much more intense (Fig. 2b). A vertical cross-section (along line B-B' in Fig. 2b), taken in the same system-relative location as the cross-section in Fig. 1c, robustly displays the elements of the canonical warm occluded thermal structure (Fig. 2c) and presents a striking

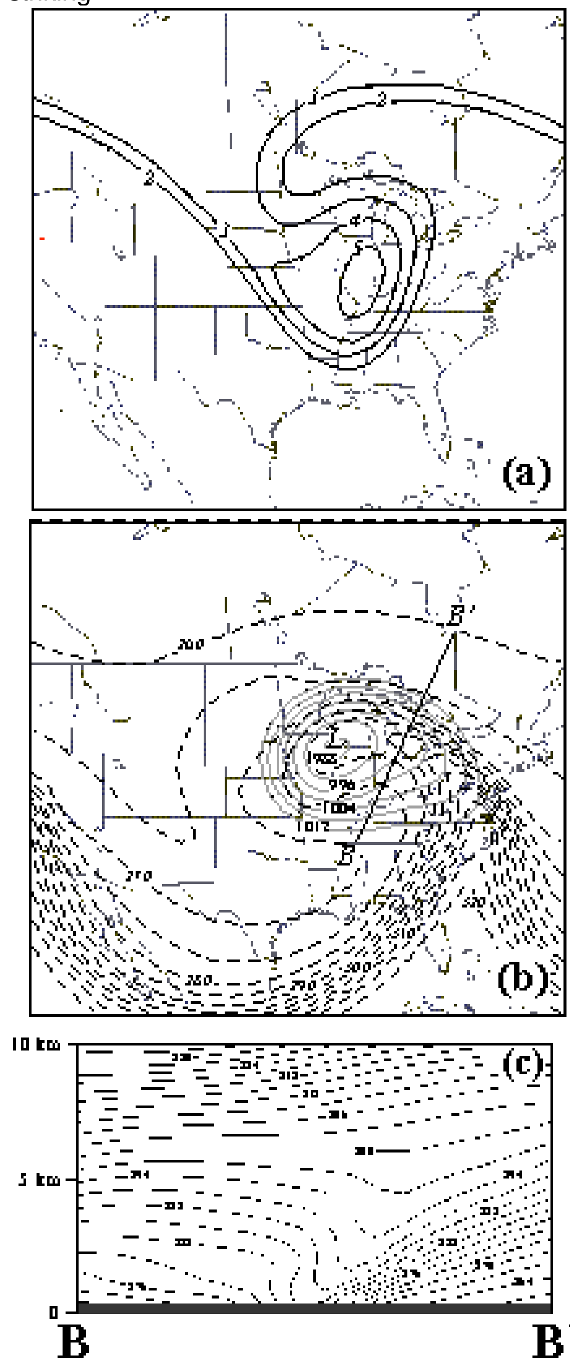

Fig. 2 (a) 9 km PV at 42 h in the FP simulation. PV labeled and contoured as in Fig. 1a. (b) Sea-level isobars (thick gray lines) and 300m θ_e (dashed lines) at 42 h in the NLHR simulation. Isobars and θ_e labeled and contoured as in Fig. 1b. (c) Vertical cross-section along line B-B' in Fig. 2b of θ_e. θ_e labeled and contoured as in Fig. 1c.

contrast to the relatively weak feature shown in Fig. 1c.

Finally, as a means of highlighting the significant differences in the tropopause-level PV between the two simulations, we show the PV difference (FP – NLHR) in Fig. 3. The

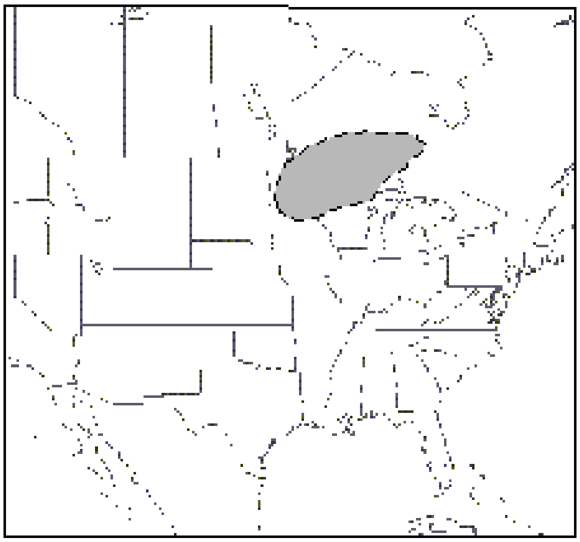

Fig. 3 9 km PV difference between the FP and NLHR simulations at 42 h. Shaded area represents region where the NLHR 9 km PV is more than 0.5 PVU larger than the FP 9 km PV.

occluded quadrant of the cyclone is the region in which the differences are most notable, reaching as high at –0.9 PVU over the far northern Minnesota.

It is clear that significant differences in both the tropopause-level PV and in the underlying tropospheric thermal structure are related to the presence of latent heat release in the FP simulation. In the conference presentation we will further explore the differences between the two simulations and illustrate the mechanisms by which these differences are made manifest.

ACKNOWLEDGEMENTS: This work is funded by a grant from the National Science Foundation (ATM-9813398).

REFERENCES

Cao, Z. and H.-R. Cho, 1995: Generation of moist potential vorticity in extratropical cyclones. *J. Atmos.Sci.*, **52**, 3263-3281.

Emanuel, K. A., 1991: A scheme for representing cumulus convection in large-scale models. *J. Atmos. Sci.*, **48**, 2313-2335.

Fritsch, J. M., E. L. Magaziner, and C. F. Chappell, 1980: Analytical initialization for three-dimensional numerical models. *J. Appl. Meteor.*, **19**, 809-818.

Martin, J. E., 1998: The structure and evolution of a continental winter cyclone. Part I: Frontal structure and the occlusion process. *Mon. Wea. Rev.*, **126**, 303-328.

Nuss, W. A. and R. A. Anthes, 1987: Numerical investigation of low-level processes in rapid cyclogenesis. *Mon. Wea. Rev.*, **115**, 2728-2743.

Posselt, D. J. and J. E. Martin, 2003: The effect of latent heat release on the evolution of a warm occluded thermal structure. *Mon. Wea. Rev.*, **131**, (accepted with revisions).

Tripoli, G. J., 1992: A nonhydrostatic model designed to simulate scale interaction. *Mon. Wea. Rev.*, **120**, 1342-1359.